Neurocomputing 74 (2011) 1301–1314

Contents lists available at ScienceDirect

Neurocomputing

journal homepage: www.elsevier.com/locate/neucom

A variational Bayesian approach for the robust analysis of the cortical silent period from EMG recordings of brain stroke patients

Iván Olier [a], Julià Amengual [b], Alfredo Vellido [c,*]

[a] School of Psychological Sciences, The University of Manchester, Zochonis Building, M13 9PL Manchester, United Kingdom
[b] Neurodynamics Laboratory, Department of Psychiatry and Clinical Psychobiology, Universitat de Barcelona, 08035 Barcelona, Spain
[c] Dept. de Llenguatges i Sistemes Informàtics - Universitat Politècnica de Catalunya, Edifici Omega, Campus Nord, 08034 Barcelona, Spain

ARTICLE INFO

Available online 22 February 2011

Keywords:
Multivariate time series
Manifold learning
Variational Bayesian generative topographic mapping
Index of variability
Electromyography
Brain stroke
Cortical silent period

ABSTRACT

Transcranial magnetic stimulation (TMS) is a powerful tool for the calculation of parameters related to the intracortical excitability and inhibition of the motor cortex. The cortical silent period (CSP) is one such parameter that corresponds to the suppression of muscle activity for a short period after a muscle response to TMS. The duration of the CSP is known to be correlated with the prognosis of brain stroke patients' motor ability. Current methods for the estimation of the CSP duration are very sensitive to the presence of noise. A variational Bayesian formulation of a manifold-constrained hidden Markov model is applied in this paper to the segmentation of a set of multivariate time series (MTS) of electromyographic recordings corresponding to stroke patients and control subjects. A novel index of variability associated to this model is defined and applied to the detection of the silent period interval of the signal and to the estimation of its duration. This model and its associated index are shown to behave robustly in the presence of noise and provide more reliable estimations than the current standard in clinical practice.

1. Introduction

The field of clinical neurology often deals with complex data that require advanced data analysis techniques with capabilities beyond those of traditional statistics. In particular, the acquisition of physiological data of motor activity resulting from cognitive processes is usually fraught with measurement artifacts and noise. This noise must be processed using robust procedures in order to extract usable knowledge. This is the case not only for the purpose of research but also for the routine medical practice.

In electromyographical (EMG) recordings, the electrical muscle activity resulting from the activity of motor neurons is recorded from the skin surface above the muscle, and not at the muscle itself, in order to avoid unnecessary discomfort in the analyzed subject. EMG recordings are very sensible to muscle activation, and it is very important to maintain the muscle in a state of relaxation during data collection. In clinical neurology research, the majority of subjects participating in the studies are patients affected by a given pathology. This often makes data acquisition, processing, and analysis rather difficult undertakings. For the reasons outlined above, physiological data in general and EMG data, which are the concern of this paper, in particular, should benefit from the development and use of data analysis models that behaved robustly in the presence of noise.

This paper analyzes data from brain stroke patients. A brain stroke is the rapidly developing loss of brain functions due to disturbance in the blood supply to the brain. The majority of stroke patients suffer motor disabilities as a result. The recovery of the motor skills strongly depends on the rehabilitation performed in the acute phase of stroke (under 6 months after stroke).

Many studies of neural plasticity in stroke patients have shown correlations between brain parameters (obtained through neuropsychological tests and brain stimulation techniques) and the prognosis of the patient (i.e., the prediction of functional recovery after the acute stroke phase). Transcranial magnetic stimulation (TMS) is a non-invasive brain stimulation method used to excite neurons. With TMS, brain activity can be triggered with minimal discomfort, and the functionality of the circuitry and connectivity of the brain can thus be studied. This technique has its more obvious application in motor cortex analysis. In brain stimulation using TMS, EMG can be used to register the signal of the corresponding muscle activation. Through this signal, several excitatory and inhibitory parameters can be studied. One of the most important inhibitory parameters is the cortical silent period (CSP) [1]. The CSP is a refractory period in the EMG signal, elicited after motor cortex stimulation with voluntary pre-activation of the target muscle.

* Corresponding author. Tel.: +34 93 413 7796.
E-mail address: avellido@lsi.upc.edu (A. Vellido).

0925-2312/$ - see front matter © 2011 Elsevier B.V. All rights reserved.
doi:10.1016/j.neucom.2010.12.006

The duration of this de-activation interval is an important parameter in the study of stroke, as research has provided evidence that the CSP shortens during the recovery of the affected limbs, making it a reliable indicator of therapeutic progress [2,3]. EMG recordings of stroke patients are often difficult in both acute and chronic patients. Some stroke patients have great difficulty in maintaining the muscle contraction in any stable way. As a result, some spurious low-amplitude EMG activity is likely to be detected during the CSP, making its analysis difficult.

Several attempts to define methods for the accurate estimation of the CSP duration have been made [4–6] with varying success. The CSP measuring methods in common use, though, are known to yield a significant error due to their sensitivity to noise, which is commonplace in this kind of data. Therefore, no fully satisfactory answer to the accurate estimation of CSP as yet been provided. This limitation calls for the development of EMG signal analysis methods capable of dealing with noise through effective regularization and, more specifically, methods for the robust estimation of the CSP in EMG recordings.

For this, we resort in this paper to a manifold-constrained hidden Markov model, which formulation within a variational Bayesian framework imbues it with regularization properties that minimize the negative effect of the presence of noise in the EMG MTS. A novel index of variability is defined for this model. It is shown to be capable of estimating the duration of the CSP by accurately pinpointing its offset time. This model and its associated index are shown in this study, through several experiments, to provide more reliable estimations than the current standard in clinical practice.

2. Medical background

2.1. Brain stroke

A stroke is the rapidly developing loss of brain functions due to disturbance in the blood supply to the brain. As a result, the affected area of the brain is unable to function. This can lead, for instance, to inability to move one or more limbs on one side of the body; to cognitive impairments such as inability to understand or formulate speech (aphasia); or to inability to perceive one side of the visual field (homonymous hemianopsia).

The prognosis of stroke patients is uncertain: About 10% of people who have an ischemic stroke recover almost all normal function, whereas about 25% recover most of it. About 40% show moderate to severe impairments requiring special care, and up to 10% require care in a nursing home or other long-term care facility. Most of the impairments that remain after 12 months become permanent.

2.2. Rehabilitation from brain stroke

Disability associated with hemiplegia or hemiparesis markedly limits independent living and social participation in at least half of all stroke survivors [7]. Reduced levels of exercise and daily activity as a consequence of the disability can increase risk factors for recurrent stroke and associated cardiovascular disease. Within days after the onset of a stroke, clinicians can begin to promote functional recovery in their patients.

Initial motor gains after stroke might result from the resolution of reversible injuries to neurons and glia. Reorganization of spared assemblies of neurons that represent motor actions within the sensorimotor cortex, as well as in transcortical, ascending and descending pathways, seems to accompany further improvements in motor skills [7]. Contributions from more widely distributed cortical and subcortical regions, including cerebral systems for perception, attention, motivation, executive planning, working memory, as well as explicit and implicit learning, may be required to compensate for strategies that the injured brain can no longer support. The ability to strengthen muscles and reach an appropriate level of cardiovascular fitness also depends on these non-motor systems.

In some animal models of stroke, M1 and related motor cortices and the spinal cord evolve robust changes in their structure and function in response to specific types of motor training. Skills training induces the creation of new synaptic connections, as well as synaptic potentiation and reorganization of movement representations within the motor cortex. This plasticity supports the production and refinement of skilled movement sequences.

The biological responses to exercise in patients are likely to depend on how long after stroke the exercise is initiated, the amount of exercise administered, and the duration and type of the task practiced by patients. In terms of improving daily functioning, task-specific training seems to benefit stroke patients more than general exercise does. One of the problems in demonstrating the specific effects in practice of any given task across rehabilitation trials has been the low intensity of training, which might limit the robustness of outcomes [8]. In addition, responsiveness to training has been observed mostly in patients who have retained reasonable motor control.

However, the effectiveness of classical approaches in rehabilitation methods, such as rehabilitation based on repetitive manipulation of objects and movement training of the affected side, has been found to be quite limited [9]. As a result, a need for efficient motor rehabilitation approaches still remains.

New rehabilitation methods, such as constraint-induced therapy, which consist on the use of the impaired extremity while immobilizing the healthy one for several hours per day, have been shown to lead to functional reorganization. In this field, animal studies have provided evidence that cortical plasticity is increased by the behavioral relevance of the stimulation and its motivational value.

2.3. Transcranial magnetic stimulation and the cortical silent period

Transcranial magnetic stimulation can be applied in several ways and at different levels of the nervous system. The TMS of the cerebral cortex is quite different from that of other parts of the nervous system: The EMG responses to cortical stimulation are more complex than those following the peripheral stimulation. Not only excitatory effects but also inhibitory effects can be elicited. This characteristic is used to investigate cerebral functions other than those of the motor cortex [10].

When an individual is instructed to maintain muscle contraction and a single supra-threshold TMS pulse is applied to the motor cortex contralateral to the target muscle, the EMG activity is arrested for a few hundred milliseconds [11]. This period of EMG suppression is referred to as a CSP, normally defined as the time from the end of the motor evoked potential (MEP) to the return of voluntary EMG activity. However, the definition of the end of the MEP is, at times, difficult. In order to circumvent this difficulty, some investigators have defined the CSP as the interval from stimulus delivery to the return of voluntary activity [12]. Silent periods of abnormally short or long duration are observed in patients with various movement disorders [13].

Classen and co-workers [14] investigated patients after acute stroke, who showed hemiparesis and a long duration of the silent period, but normal MEP amplitude in the affected side. These patients had impaired movement initiation, inability to maintain a constant force, and impaired movement of individual fingers that resembled motor neglect. The CSP duration decreased with clinical improvement.

Most reports seem to agree that the threshold for evoking a CSP is relatively stable in patients, especially if expressed as relative to motor threshold intensities. However, the duration of the CSP is prolonged, at least in the acute phase of the affected site. Traversa et al. [15] showed that the CSP shortens during recovery and there is some suggestion that the amount of such shortening correlates with the recovery of hand function [16]. More recent studies support this correlation as a good prognostic indicator and, thus, as a good indicator of the capabilities of the therapy [17,18]. However, this shortening of the CSP is strongly dependent on the type of chosen rehabilitation therapy.

2.4. The current standard for the estimation of the CSP duration

Alternative techniques for the estimation of the CSP have been developed over the last few years [5,6], but they still lack sufficient clinical testing. The current standard for the automated calculation of the CSP offset was developed by Daskalakis et al. [4]. In this automated approach (hereafter referred to as Daskalakis method, or DM for short), a combination of filtering, squaring and threshold detection is used to calculate the CSP duration. The method has the advantage of being objective, as it avoids the potential biases and interpretation discrepancies inherent to previously proposed, more conventional and visually guided CSP measuring techniques. It has also been widely accepted for its simplicity of implementation, which is accessible to people with little or no computational background.

In DM, the end of the CSP is marked by the first return of any voluntary EMG activity, defined as the first time point at which the background EMG returns to 25% of pre-stimulus EMG amplitude.

Despite the reliability of this method to automate the determination of the CSP at short or long durations, its main limitations reside, first, in the inability to cope with more complex CSP cases where additional CSPs follow bursts of EMG activity; and second, in its bad performance in the presence of noisy data, which are commonplace in pathological EMG recordings.

While acquiring the EMG signal from patients who are not able to maintain a voluntary muscle contraction, or who suffer some sickness related to muscle control, spontaneous EMG activity during the CSP is likely to occur. This activity is not relevant to the analysis, as it is not related with disinhibition of pyramidal cells. DM cannot distinguish these cases. Moreover, the 50 Hz high-pass filtering procedure applied in this technique sometimes hides relevant EMG signal information related to the return of the voluntary contraction, and can result in an unreliable calculation of the CSP.

3. Variational Bayesian GTM-TT and its use for the estimation of the CSP duration

Finding low-dimensional representations of multivariate data that reside in high-dimensional data spaces is a problem that concerns machine learning and pattern recognition. Latent variable models [19] address this problem by representing information from an observable data space in an unobservable or latent, usually low-dimensional, space. In [20], these models are typified as belonging to different but overlapping categories: projection models, generative models, and other related models.

Projection models aim to project data points residing in $\Re^D$ onto a hyperplane, $\Re^L$, with $\Re^L \subseteq \Re^D$, where $L \leq D$. The most commonly used projection model is principal component analysis (PCA) [21], although other models, such as principal curves and surfaces [22], auto-associative feed-forward neural networks [23], and kernel based PCA [24], are also of common use.

Generative models are defined stochastically and try to estimate the distribution of data by defining a density model with low intrinsic dimensionality within the multivariate data space. Possibly, factor analysis (FA) [25,26] is the most widely used generative model. This type of models fit naturally into the statistical machine learning category and, in general, into the wider framework of probability theory and statistics.

Generative topographic mapping (GTM) is a nonlinear generative model introduced in [27]. In short, it was defined to retain all the useful characteristics of Kohonen's self-organizing maps (SOM) [28], such as the simultaneous clustering and visualization of multivariate data, while eluding most of its limitations through a fully probabilistic formulation. Such formulation has enabled the definition of principled extensions for hierarchical structures [29], missing data imputation [30], adaptive regularization [31,32], discrete data modelling [33,34], robust outlier detection and handling [35], and semi-supervised learning [36], amongst others.

GTM-through time (GTM-TT) [37] is an extension of GTM suited to deal with the unsupervised analysis of MTS. Given that it is defined as a constrained hidden Markov model (HMM) [38], GTM-TT explicitly accounts for the violation of the independent identically distributed (i.i.d) condition. This model has been assessed using artificial and real MTS in [39].

In this section, we first describe the original GTM and its extension to the modelling of MTS: GTM-TT. A Bayesian approach to the definition of GTM-TT is then outlined. This Bayesian formulation should deal effectively with the problem of overfitting. Finally, a recently developed variational approach for Bayesian GTM-TT [40] is summarily introduced.

3.1. The original GTM

The neural network-inspired GTM is a nonlinear latent variable model of the manifold learning family with sound foundations in probability theory. It performs simultaneous clustering and visualization of the observed data through a nonlinear and topology-preserving mapping from a visualization latent space in $\Re^L$ (with L being usually 1 or 2 for visualization purposes) onto a manifold embedded in the $\Re^D$ space, where the observed data reside.

The mapping that generates the manifold is carried out through a generalized regression function, given by $\mathbf{y} = \mathbf{W}\boldsymbol{\Phi}(\mathbf{u})$, where $\mathbf{y} \in \Re^D$, $\mathbf{u} \in \Re^L$, $\mathbf{W}$ is the matrix that generates the mapping, and $\boldsymbol{\Phi}$ is a matrix with the images of S basis functions ϕ_s (defined as radially symmetric Gaussians in the original formulation of the model). The prior distribution of $\mathbf{u}$ in latent space is constrained to form a uniform discrete grid of K centers, analogous to the layout of the SOM units, in the form of a sum of delta functions: $p(\mathbf{u}) = (1/K)\sum_{k=1}^{K} \delta(\mathbf{u}-\mathbf{u}_k)$.

This way defined, GTM can also be understood as a constrained mixture of distributions (Gaussians in the standard model). That is, a special case of a mixture model that is adapted to provide high-dimensional data visualization. Assuming that the observed data set $\mathbf{X}$ is constituted by N independent, identically distributed (i.i.d.) data points $\mathbf{x}_n$, leads to the definition of a complete likelihood in the form:

$$p(\mathbf{X}|\mathbf{W},\beta) = \left(\frac{\beta}{2\pi}\right)^{ND/2} \prod_{n=1}^{N} \left\{ \frac{1}{K} \sum_{k=1}^{K} \exp\left(-\frac{\beta}{2} \|\mathbf{x}_n - \mathbf{y}_k\|^2 \right) \right\} \quad (1)$$

where $\mathbf{y}_k = \mathbf{W}\boldsymbol{\Phi}(\mathbf{u}_k)$.

The adaptive parameters of the model, which are $\mathbf{W}$ and the common inverse variance of the Gaussian components, β, are usually optimized by maximum likelihood (ML) using the expectation–maximization (EM) algorithm [41]. Details of this calculations can be found in [27].

As mentioned, the GTM is embodied with clustering and visualization capabilities that are akin those of the SOM. For instance, and

as used later in the article, data points can be summarily visualized in the low-dimensional latent space (of 1 or 2 dimensions) of GTM by means of the *posterior-mode* projection [31], defined as $k_n^{mode} = \text{argmax}_{\{k_n\}} p(\mathbf{u}_k|\mathbf{x}_n)$, which also provides an assignment of each data point $\mathbf{x}_n$ to a cluster representative $\mathbf{u}_k$.

3.2. The GTM through time

The data mining of MTS has long ago become an established research area [42]. Methods dealing with this problem have stemmed from both traditional statistics and machine learning field, using neural networks as a fruitful approach [43].

These methods usually consider the problem as supervised, prediction being the main goal of the analysis. In comparison, little research has been devoted to methods of unsupervised clustering for the exploration of the dynamics of MTS.

Some of the most interesting time series clustering results have been obtained with different variants of SOM models in diverse contexts although, in general, without accounting for the violation of the i.i.d condition.

The GTM-TT [37] is an extension of GTM suited to deal with the unsupervised analysis of MTS. It explicitly accounts for the violation of the i.i.d. condition, given that it is defined as a constrained HMM.

GTM-TT can be considered as a GTM model in which the latent states are linked by transition probabilities, in a similar fashion to hidden Markov models. In fact, GTM-TT can be understood as a topology constrained HMM.

Assuming a sequence of N hidden states $\mathbf{Z} = \{z_1, z_2, \ldots, z_n, \ldots, z_N\}$ and the observed MTS $\mathbf{X} = \{\mathbf{x}_1, \mathbf{x}_2, \ldots, \mathbf{x}_n, \ldots, \mathbf{x}_N\}$, the probability of the observations is given by

$$p(\mathbf{X}) = \sum_{\text{all } \mathbf{Z}} p(\mathbf{Z},\mathbf{X}) \tag{2}$$

where $p(\mathbf{Z},\mathbf{X})$ defines the complete-data likelihood as in HMM models [38] and takes the following form:

$$p(\mathbf{Z},\mathbf{X}) = p(z_1) \prod_{n=2}^{N} p(z_n|z_{n-1}) \prod_{n=1}^{N} p(\mathbf{x}_n|z_n) \tag{3}$$

The model parameters are $\mathbf{\Theta} = (\boldsymbol{\pi},\mathbf{A},\mathbf{Y},\beta)$ where $\boldsymbol{\pi} = \{\pi_j\} : \pi_j = p(z_1 = j)$ are the initial state probabilities, $\mathbf{A} = \{a_{ij}\} : a_{ij} = p(z_n = j|z_{n-1} = i)$ are the transition state probabilities, and

$$\{\mathbf{Y},\beta\} : p(\mathbf{x}_n|z_n = j) = \left(\frac{\beta}{2\pi}\right)^{D/2} \exp\left(-\frac{\beta}{2}\|\mathbf{x}_n - \mathbf{y}_j\|^2\right)$$

are the emission probabilities, which are controlled by spherical Gaussian distributions with common inverse variance β and a matrix $\mathbf{Y}$ of K centroids $\mathbf{y}_j$, $1 \le j \le K$.

For mathematical convenience, it is useful defining a state in the vectorial form $\mathbf{z}_{j,n}$ such that it returns 1 if z_n is in state j, and zero otherwise. Using this notation, the initial state probabilities, the transition state probabilities and the emission probabilities are defined as

$$p(z_1|\boldsymbol{\pi}) = \prod_{j=1}^{K} \pi_j^{\mathbf{z}_{j,1}} \tag{4}$$

$$p(z_n|z_{n-1},\mathbf{A}) = \prod_{i=1}^{K}\prod_{j=1}^{K} a_{ij}^{\mathbf{z}_{j,n}\mathbf{z}_{i,n-1}} \tag{5}$$

$$p(\mathbf{x}_n|z_n,\mathbf{Y},\beta) = \left(\frac{\beta}{2\pi}\right)^{D/2} \prod_{j=1}^{K} \left\{\exp\left(-\frac{\beta}{2}\|\mathbf{x}_n - \mathbf{y}_j\|^2\right)\right\}^{\mathbf{z}_{j,n}} \tag{6}$$

Eqs. (4) and (6) lead to the definition of the complete data log-likelihood $\ln p(\mathbf{Z},\mathbf{X}|\mathbf{\Theta})$, and parameter estimation can be accomplished in GTM-TT by maximum likelihood using the EM algorithm, in a similar fashion to HMMs. Details can be found in [37].

3.3. Bayesian GTM through time

Although the ML framework is widely used for parameter optimization, it shows two important weakness:

- Its maximization process does not take into account the model complexity.
- It tends to overfit the model to the training data.

The complexity in GTM-TT data representation is modulated by several parameters, such as the number of hidden states, their degree of connectivity and the dimension of the hidden space. For visualization processes, the dimension of the hidden space is limited to be three or less. The number of hidden states and the maximum number of possible state transitions are strictly correlated by a squared power. In order to solve the overfitting problem, the complexity has been limited by restricting the number of possible state transitions [37] or by fixing the transition state probabilities a priori [44]. The alternative technique of cross-validation is computationally very expensive and it requires large amounts of data to obtain low-variance estimates of the expected test errors. To control overfitting and model complexity, a full Bayesian reformulation of GTM-TT was recently proposed: The variational Bayesian GTM-TT (henceforth VBGTM-TT [40,45]).

The Bayesian approach treats the parameters as unknown quantities and provides probability distributions for their priors. Bayes' theorem can be used to infer the posterior distributions over the parameters. The model parameters can thus be considered as hidden variables and integrated out to describe the marginal likelihood as

$$p(\mathbf{X}) = \int p(\mathbf{\Theta}) p(\mathbf{X}|\mathbf{\Theta}) d\mathbf{\Theta} \quad \text{where } \mathbf{\Theta} = (\pi,\mathbf{A},\mathbf{Y},\beta) \tag{7}$$

If an independent distribution is assumed for each parameter, then

$$p(\mathbf{\Theta}) = p(\boldsymbol{\pi})p(\mathbf{A})p(\mathbf{Y})p(\boldsymbol{\beta}) \tag{8}$$

Taking into account Eqs. (2), (7) and (8), the marginal likelihood in GTM-TT can be expressed, similarly to HMM [46], as

$$p(\mathbf{X}) = \int p(\boldsymbol{\pi}) \int p(\mathbf{A}) \int p(\mathbf{Y}) \int p(\beta) \sum_{\text{all } \mathbf{Z}} p(\mathbf{Z},\mathbf{X}|\boldsymbol{\pi},\mathbf{A},\mathbf{Y},\beta)\, d\beta\, d\mathbf{Y}\, d\mathbf{A}\, d\boldsymbol{\pi} \tag{9}$$

Although there are many possible prior distributions to choose from, the conjugates of the distributions defined in Eqs. (4) and (6) are a reasonable choice. In this way, a set of prior distributions is defined as follows:

$$p(\boldsymbol{\pi}) = \texttt{Dir}(\{\pi_1, \ldots, \pi_K\}|\boldsymbol{\nu})$$

$$p(\mathbf{A}) = \prod_{j=1}^{K} \texttt{Dir}(\{a_{j1}, \ldots, a_{jK}\}|\boldsymbol{\lambda})$$

$$p(\mathbf{Y}) = [(2\pi)^K|\mathbf{C}|]^{-D/2} \prod_{d=1}^{D} \exp\left(-\frac{1}{2}\mathbf{y}_{(d)}^T \mathbf{C}^{-1} \mathbf{y}_{(d)}\right)$$

$$p(\beta) = \Gamma(\beta|d_\beta, s_\beta)$$

where $\texttt{Dir}(\cdot)$ represents the Dirichlet distribution; and $\Gamma(\cdot)$ is the Gamma distribution. The vector $\boldsymbol{\nu}$, the matrix $\boldsymbol{\lambda}$ and the scalars d_β and s_β correspond to the hyperparameters of the model which are fixed *a priori*. The prior over the parameter $\mathbf{Y}$ defines the mapping from the hidden states to the data space as a Gaussian process

(GP), where $\mathbf{y}_{(d)}$ is each of the row vectors (centroids) of the matrix $\mathbf{Y}$ and $\mathbf{C}$ is a matrix where each element is a covariance function that can be defined as

$$C(\mathbf{u}_i,\mathbf{u}_j) = v\exp\left(-\frac{\|\mathbf{u}_i-\mathbf{u}_j^2}{2\alpha^2}\right), \quad i,j=1\ldots K \tag{10}$$

The α parameter controls the flexibility of the mapping from the latent space to the data space. The vector $\mathbf{u}_j, j=1\ldots K$ corresponds to the state j in a latent space of usually lower dimension than that of the data space. Thus, a topography over the states is defined by the GP as in the standard GTM.

A graphical model representation of the proposed Bayesian GTM-TT can be seen in Fig. 1.

Unfortunately, Eq. (9) is analytically intractable. In the following subsection, we provide the details of its approximation using variational inference techniques.

3.4. A variational approach for Bayesian GTM-TT

Variational inference allows approximating the marginal log-likelihood through Jensen's inequality as follows:

$$\begin{aligned}\ln p(\mathbf{X}) &= \ln \int \sum_{\text{all } \mathbf{Z}} p(\mathbf{Z},\mathbf{X}|\boldsymbol{\Theta})p(\boldsymbol{\Theta})\, d\boldsymbol{\Theta} \\ &\geq \int \sum_{\text{all } \mathbf{Z}} q(\boldsymbol{\Theta},\mathbf{Z}) \ln \frac{p(\mathbf{Z},\mathbf{X}|\boldsymbol{\Theta})p(\boldsymbol{\Theta})}{q(\boldsymbol{\Theta},\mathbf{Z})}\, d\boldsymbol{\Theta} \\ &= F(q(\boldsymbol{\Theta},\mathbf{Z}))\end{aligned}$$

The function $F(q(\boldsymbol{\Theta},\mathbf{Z}))$ is a lower bound such that its convergence guarantees the convergence of the marginal likelihood. The goal in variational inference is choosing a suitable form for the approximate density $q(\boldsymbol{\Theta},\mathbf{Z})$ in such a way that $F(q)$ can be readily evaluated and yet which is sufficiently flexible that the bound is reasonably tight. A reasonable approximation for $q(\boldsymbol{\Theta},\mathbf{Z})$ is based on the assumption that the hidden states $\mathbf{Z}$ and the parameters $\boldsymbol{\Theta}$ are independently distributed, i.e. $q(\boldsymbol{\Theta},\mathbf{Z}) = q(\boldsymbol{\Theta})q(\mathbf{Z})$. Thereby, a variational EM algorithm can be derived [46]:

VBE-step:

$$q(\mathbf{Z})^{(\text{new})} \leftarrow q(\mathbf{Z}) \underset{q(\mathbf{Z})}{\operatorname{argmax}} F(q(\mathbf{Z})^{(\text{old})}, q(\boldsymbol{\Theta})) \tag{11}$$

VBM-step:

$$q(\boldsymbol{\Theta})^{(\text{new})} \leftarrow q(\boldsymbol{\Theta}) \underset{q(\boldsymbol{\Theta})}{\operatorname{argmax}} F(q(\mathbf{Z})^{(\text{new})}, q(\boldsymbol{\Theta})) \tag{12}$$

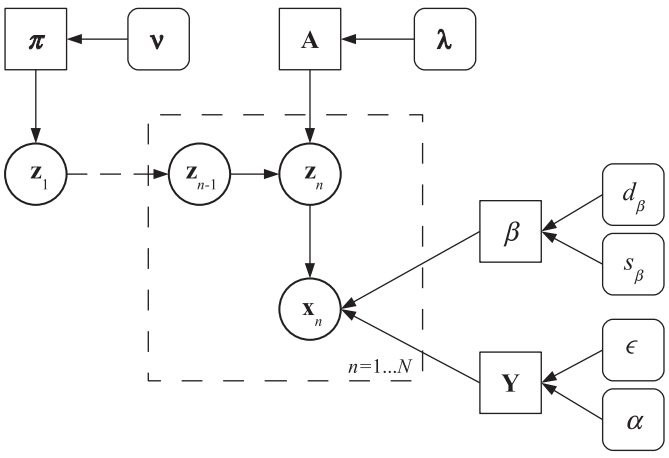

Fig. 1. Graphical model representation of the Bayesian GTM-TT. Variables are noted by circles, parameters, by squares and hyperparameters, by rounded squares.

The model is implemented by these two equations. Details of such implementation can be found in [45].

3.5. A novel approach to the estimation of the CSP duration: the index of variability

The GTM-TT model, described in the previous subsections, can facilitate the faithful identification and visualization of change-points and sudden transitions in MTS [40]. Change-points, in the low-dimensional visual data representation provided by the model, correspond to sudden jumps between often distant model states. Instead, subsequences of little variability over time will often clump in few model states or even remain in a single one over time.

In this study, we hypothesize that the CSP can be encapsulated by change points. In other words, we claim that the GTM-TT model should be able to unambiguously identify the CSP as a time subsequence of little variability, bounded by change points.

To test such hypothesis, and beyond the exploratory visualization of MTS that GTM-TT can provide, we need a well-defined measure of MTS variation that allows us to identify and quantify change-points. In GTM-TT, we expect sudden transitions to be accompanied by sudden increases of the model likelihood [47], so that the weighted mean of the emission probabilities of the model in logarithmic form could be a good candidate to consider as an index of variability (*IV*):

$$IV_n = -\sum_k r_{k,n} \ln p(\mathbf{x}_n|\mathbf{z}_n = k)$$

where $r_{k,n} = p(\mathbf{z}_n = k|\mathbf{x}_n)$ is the responsibility (a posterior probability) taken by a hidden state $z_n = k$ out of K for each point $\mathbf{x}_n$ in the MTS.

Unfortunately, this measure can be affected by noise, and it will not reflect the advantages of the data regularization provided by the VB-GMT-TT. For this reason, a novel *IV*, namely the weighted-prototype *IV* (*wpIV*), is proposed for the latter model and defined as

$$wpIV_n = \|\Omega_n^{mean} - \Omega_{n-1}^{mean}\| \tag{13}$$

where $\|\cdot\|$ is the Euclidean distance and $\Omega_n^{mean} = \sum_{k=1}^{K} \langle z_{k,n} \rangle \mathbf{y}_k$. Here, the variational parameter $\langle z_{k,n} \rangle$ plays the same role as $r_{k,n}$ plays for the standard GTM-TT, and vector $\mathbf{y}_k$; $k=1\ldots K$ is the data prototype of state k in data space. Eq. (13) is nothing but the weighted distance between the data prototypes representing two consecutive instants in the MTS, where each prototype can take at least partial responsibility for the representation of each instant of the MTS. The same distance measured between the observed data of the two consecutive instants would be of little use as any relevant information would be masked by noise.

By measuring the distance using the model-generated prototypes, we ensure that, provided the model manages to faithfully recover the underlying structure of the MTS (and VB-GTM-TT does this by avoiding overfitting while the standard GTM-TT cannot), the true change-points will be clearly detected.

4. Experiments and discussion

4.1. Experimental settings

The previous sections should provide the boundaries for our experiments. Given that we are proposing a new technique – based on a novel statistical machine learning model – that might be useful to estimate the duration of the CSP in general

neurological and psychiatric disorders, the experimental procedure is set as follows:

- First, fully synthetic data that simulate simple MTS are employed for a preliminary assessment of the adequacy of the proposed *wpIV* measure. For that, a number of increasing levels of noise are used to contaminate the original data. This way, we should be able to assess if the proposed model and the corresponding index are capable of discovering the underlying true data structured without being affected by the added noise.
- Second, synthetic data that simulate the real EMG that are the ultimate target of the current study are generated. These data are used with a twofold objective: validating the previous results with artificial MTS and comparing the performance of the proposed method with that of the current standard in the field, DM, in the presence of increasing levels of uninformative noise.
- Third, having validated the proposed *wpIV* measure with artificial data, we proceed to test it with real EMG data from control healthy patients (multiple trials per subject), who did not undergo any type of motor rehabilitation, again comparing its performance with DM.
- Fourth, the duration of the CSP is likely to vary in pathological subjects undergoing rehabilitation. Our last set of experiments is aimed to provide the first preliminary evidence that the proposed *wpIV* is a suitably robust method for the estimation of the CSP in patients undergoing rehabilitation from stroke.

Overall, these experiments are expected to be the starting point for research involving other types of neurological disorders.

4.2. EMG data

For the experiments concerning human controls, 14 voluntary healthy right-handed subjects (eight women and six men, mean age ($\pm$standard deviation) of 24.9 ($\pm$2.5) years) gave their consent to the study. They were informed about the experimental procedure and remained naïve about the aim of the study.

TMS of the right M1 was produced using a biphasic Magstim Rapid 2 (Magstim Co., Withland, Dyfed, UK), with a 8-shaped coil (external diameter of each loop 9 cm). EMG signals were acquired using surface electrodes in a belly-tendon montage from the first dorsal interoseus (FDI) muscle of the right hand.

A total of 15 trials per subject were recorded, and intervals between two consecutive TMS pulses were of at least 7 s, in order to avoid possible slow repetitive effects. Each signal covered an interval from 100 ms pre-stimulus to 500 ms post-stimulus. Subjects were not able to visually monitor the EMG signal, in order to avoid feedback effects due to the appearance of the signal.

For the experiments concerning pathological subjects, eight chronic stroke patients (three women and five men, mean age ($\pm$standard deviation) of 64.9 ($\pm$10.5) years old) were identified and recruited by examining case-records from Bellvitge Hospital at Hospitalet de Llobregat, Barcelona, Spain. All patients had suffered from first-ever ischemic stroke causing upper limb weakness (3.5–4.5 on the Medical Research Council scale). They were able to move the affected arm and the index finger without help from the healthy side.

Brain stimulation using TMS was performed using a focal air-cooled 8-shaped coil (9 cm diameter each wing) attached to a biphasic Magstim Rapid 2 Stimulator. MEPs were obtained from the FID muscle of the hand contralateral to the stimulated hemisphere. Both affected and unaffected hemispheres were tested in each session. For the CSP assessment, 15 trials were recorded for each subject, and intervals between two consecutive TMS pulses were again of a duration of at least 7 s, to avoid possible slow repetitive effects. The trial time window was pulse-locked and the length of the EMG window was adapted to the patients, being the same for all of them.

4.3. Experimental results and discussion

According to the experimental settings outlined above, the current section is structured in four parts. The first one reports the results corresponding to the experiments with synthetic general MTS. The second part reports the comparative results with synthetic data sets that emulate the typical EMG signal for the problem at hand. The third one reports results with real data of human controls. Finally, the last part offers preliminary results of experiments with real pathological subjects. In both third and fourth experiments, significance of the differences between the results obtained by both methods was tested using Cronbach's alpha [48]. Cronbach's alpha values above 0.85 were taken to indicate significant differences. Furthermore, a paired sample *t*-test was applied to test the null hypothesis consisting of the equivalence of the results obtained by both methods.

4.3.1. Validation of the wpIV: basic experiments with artificial data

The first set of experiments is meant to show the adequacy and usefulness of the *wpIV* defined above. For that, we model a simple artificial set of MTS using both the standard GTM-TT and the VB-GTM-TT.

This basic data set consists of three time series built as a piecewise combination of step-like functions concatenating four periods of constant signal through three sudden transition change-points. The signal is contaminated with increasing levels of uninformative Gaussian noise (with standard deviations of, in turn: 0.01, 0.05 and 0.1; see Fig. 2, left hand-side column).

The *wpIV* for both models and for the three noise levels is depicted in Fig. 2 (center and right columns). At the lowest noise level (top row), the *wpIV* corresponding to both models captures both the transitions and the periods of noise-related variability pretty well. At higher levels of noise, though, only the VB-GTM-TT (rightmost column) is able to keep modelling both of them faithfully. The *wpIV* for the standard GTM-TT (center column), instead, clearly reveals that the model is overfitting the data, rendering the index useless for MTS segmentation through change-point detection.

This provides the first evidence of the robustness of the VB-GTM-TT model in the presence of noise. The standard GTM-TT overfits the MTS, while its alternative formulation within a variational Bayesian framework is capable of retrieving the original underlying model with accuracy, making the estimation of the *wpIV* more faithful than that rendered by an unregularized technique.

4.3.2. Experiments with EMG-like synthetic data

We now step forward in terms of experimental complexity, getting closer to the real EMG data that are the goal of the thesis. In this experiment, we compare the performances of DM and VB-GTM-TT using artificial MEP-like data with added noise. We do so in order to gauge the strength of both methods when faced with noisy data.

The DM was implemented in Matlab (The MathWorks^{TM}) to identify the onset and the end of the CSP using mathematical criteria. The method involves a high-pass filtering process, as well as squaring and threshold detection. All trials were high-pass filtered (suppressing waveform activity below 50 Hz) attempting to remove movement artifacts from the recordings.

The underlying artificial signal was piecewise-defined. Uninformative white noise was then generated and added to the CSP interval. The noise was used in three different settings:

1. Varying the number of trials corrupted by noise, i.e., the ratio of noisy MTS in the data set. Increasing levels of noise, with standard deviations of, in turn: 0.25, 0.5 and 1, were used.

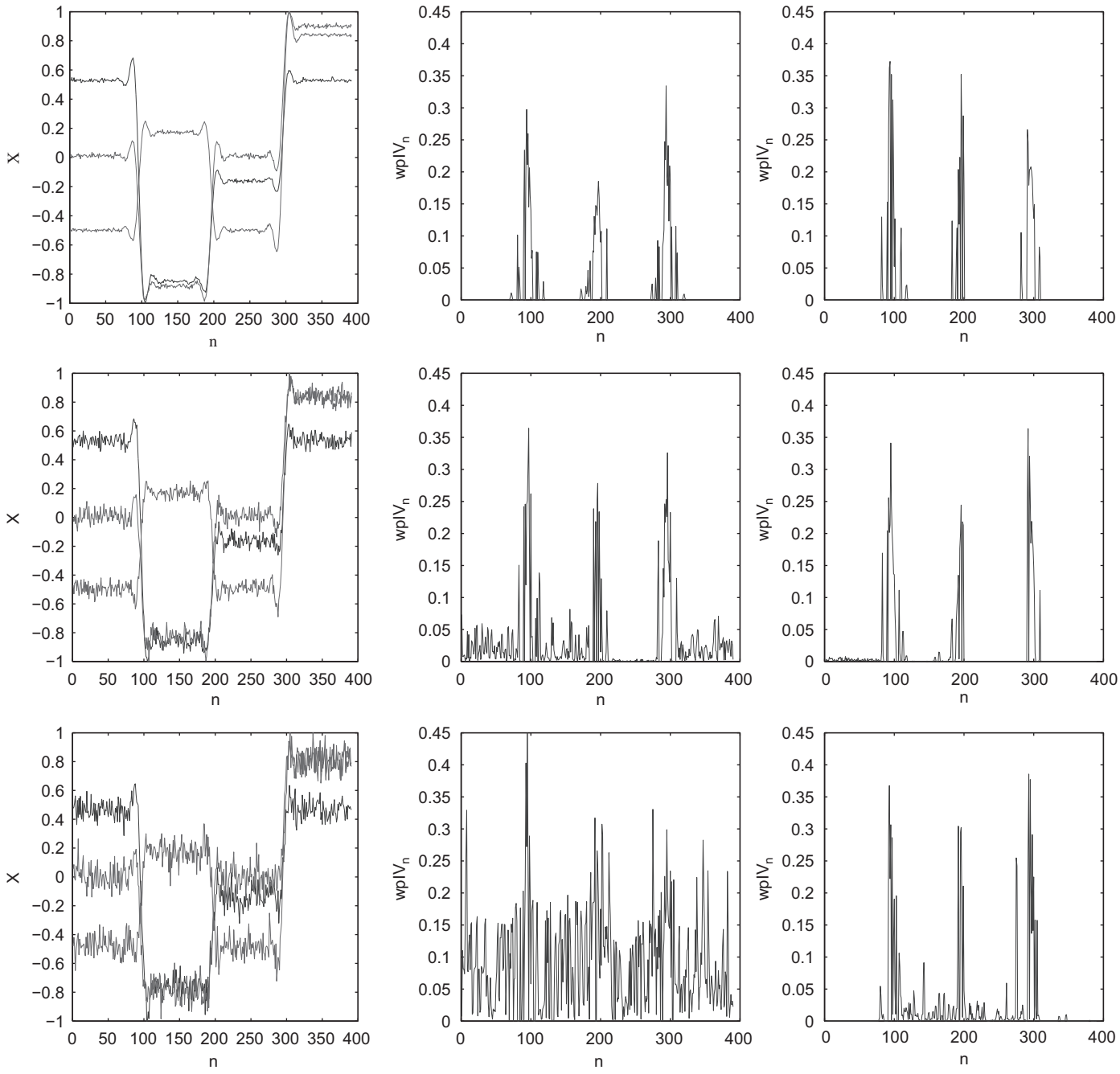

Fig. 2. *wpIV* for the artificial data at three noise levels of standard deviations: 0.01 (top row), 0.05 (middle) and 0.1 (bottom). The data are represented on the left column; the center column shows *wpIV* results for GTM-TT; and the rightmost one, for VB-GTM-TT.

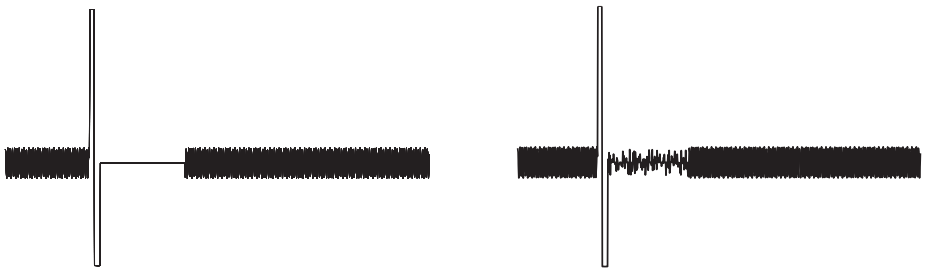

Fig. 3. (Left) Artificial data created to simulate a typical CSP. (Right) The same artificial data with white noise added to the CSP interval.

2. Modifying the amplitude of the noise generated at the CSP, with increasing values of 0.2, 0.4 and 0.6 standard deviation (see Fig. 3 for illustration).
3. Varying the number of time points corrupted by noise at the CSP, i.e., the ratio of noisy time points in the CSP, with values 0.4, 0.7, 0.9 (see Fig. 4).

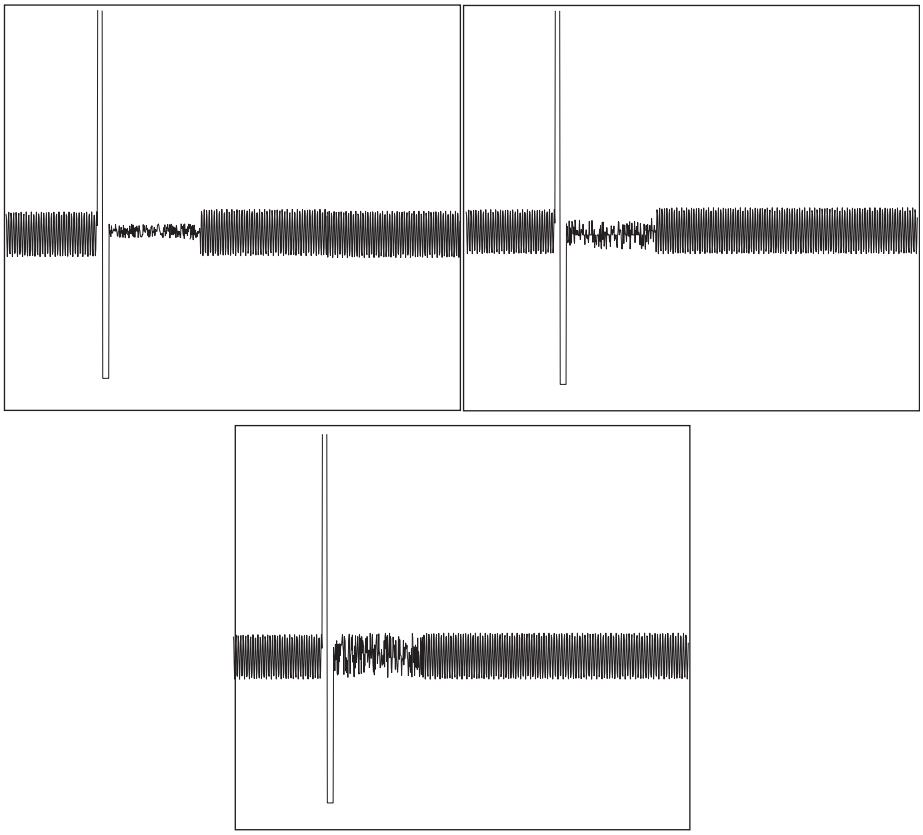

Fig. 4. Three examples of synthetic data individual trials that simulate the real EMG, in the presence of increasing levels of uninformative noise. This time, the ratio of noisy points in the silent period in each one is high (0.9), while the noise amplitude varies: 0.2 (top left), 0.4 (top right) and 0.6 (bottom).

Before and after the simulated CSP, the signal is defined as a high-frequency sinusoidal signal that emulates the voluntary muscle contraction that has to be performed by the subject.

A total of 27 noisy data sets were generated (Fig. 4), accounting for the three possible settings described above. For each data set, 15 trials were generated and analyzed by DM and the VB-GTM-TT *wpIV*. In all data sets, the offset of silent period was homogeneously established at point 426 of the simulated signal, in order to facilitate the assessment of both methods.

A full report of the results can be found in Table 1. It reveals that VB-GTM-TT was able to measure correctly the offset of the CSP in all contaminated data sets. However, DM was only able to measure correctly the offset when the noise amplitude was low. An illustration of this can be found in Fig. 5. These are very interesting results in two ways: First, VB-GTM-TT seems to be robust in the presence of noise, and second, the weakness of DM seems to be more related to the amplitude of noise located on the silent period than to either the number of trials corrupted by noise, or to the ratio of corrupted points in each trial. In any case, since the VB-GTM-TT also correctly estimates the offset of the CSP for the noise-free data set, these results provide, overall, further evidence that the *wpIV* calculated through VB-GTM-TT is a reliable tool for automating the determination of the CSP duration, specially in EMG recordings with high levels of noise.

Table 1
Mean CSP offset estimation for both models in all experimental settings described in the text.

Trials corrupted (%)	Points corrupted (%)	Noise amplitude	DM (samples)	*wpIV* (samples)
25	40	0.2	426	426
25	40	0.4	394	426
25	40	0.6	401	426
25	70	0.2	426	426
25	70	0.4	393	426
25	70	0.6	417	426
25	90	0.2	426	426
25	90	0.4	401	426
25	90	0.6	417	426
50	40	0.2	426	426
50	40	0.4	378	426
50	40	0.6	345	426
50	70	0.2	426	426
50	70	0.4	360	426
50	70	0.6	392	426
50	90	0.2	426	426
50	90	0.4	360	426
50	90	0.6	351	426
100	40	0.2	426	426
100	40	0.4	306	426
100	40	0.6	303	426
100	70	0.2	426	426
100	70	0.4	302	426
100	70	0.6	301	426
100	90	0.2	426	426
100	90	0.4	303	426
100	90	0.6	301	426

4.3.3. Experiments with control subjects

We now progress to experimentation with real data acquired from human subjects. One of the main characteristics of this set of experiments is that we do not know the true duration of the CSP any longer. This means that there is no longer a true benchmark against which to compare the performance of the analyzed techniques.

The subjects involved in these experiments were voluntary controls, unaffected by the studied pathology and, therefore, not undergoing any therapy. These data were acquired with experimental purposes unrelated to any neurological injury.

Our hypothesis is that, since voluntary control data sets should in general not be contaminated by measurement noise, the

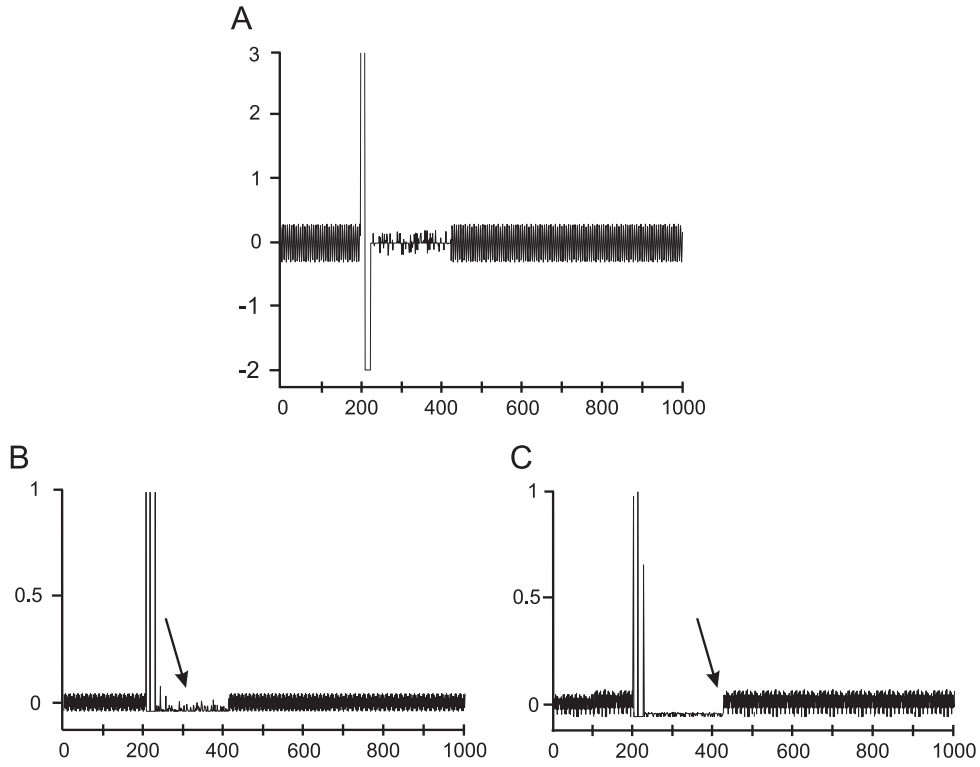

Fig. 5. (A) Artificial data created to simulate a typical CSP pattern with Gaussian noise added to the CSP interval. (B) Normalized DM output after the squaring and filtering of the data represented in (A). (C) Normalized output of the *wpIV* obtained from the data represented in (A). The arrows mark the estimations of the CSP offset in each method. DM clearly selects a wrong offset location.

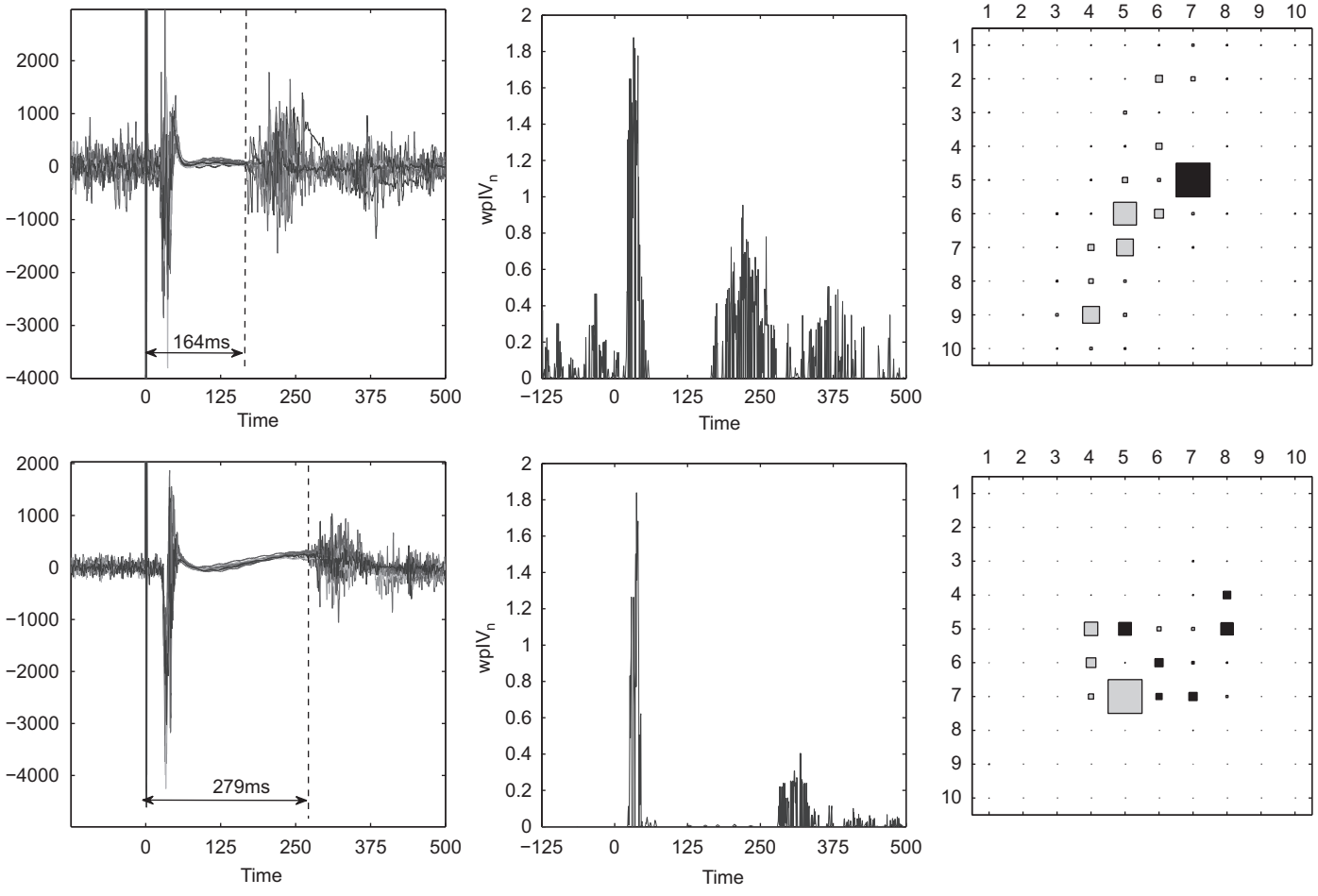

Fig. 6. (Left) Visualization of the 15 EMG MTS corresponding to the complete sets of trials for two control subjects. Dashed lines delimit the CSP durations of 164 ms (top) and 279 ms (bottom) that were estimated using the *wpIV*. (Middle) *wpIV* for these subjects. (Right) Visualization of the MTS in the VB-GTM-TT 2-D representation map. Squares represent model states and their size is an indication of the number of time points (as a ratio) assigned to each state. Such assignment takes the form of a mode-projection according to the expression $k_n^{mode} = \text{argmax}_{\{k_n\}} \langle z_{k,n} \rangle$. States filled in black correspond to the CSP.

estimations of the CSP duration yielded by DM and the VB-GTM-TT-based *wpIV* will be quite similar.

All trials for each subject were analyzed to determine the offset and the duration of the CSP, again using DM (with the previously described settings) and the VBGTM-TT-based *wpIV*. The squaring of the trace was employed to magnify and rectify the EMG activity as well as further isolate the MEP and the EMG flat period. The CSP onset was determined by the stimulus onset. The CSP offset was determined from the processed waveform and was the first point to exceed 25% of the mean pre-stimulus EMG amplitude within a generous window (between 100 and 500 ms after TMS stimulus) that consistently enclosed the flat period after the end of the MEP.

All subjects completed the TMS protocol without difficulty. In almost all subjects, all trials passed a basic quality control. In three subjects, less than three trials were discarded from the analysis because of a strong contamination by movement artifact.

The similarity of the results yielded by both methods was tested using Cronbach's alpha, resulting in a value of 0.95. No significant values for the *t*-test were found ($t(13) = -0.391$, $p > 0.7$), corroborating the lack of significant differences between the results of both estimations.

For illustration, we report next the results for two control subjects. Fig. 6 (left) shows their complete EMG. The corresponding estimation of the *wpIV* is superimposed. The *wpIV*, displayed in Fig. 6 (center), provides a completely clean-cut delimitation of the CSP that allows the unambiguous estimation of its duration.

As explained in the previous sections, one of the unique advantages of a manifold learning method such as VB-GTM-TT is that it can provide a low-dimensional intuitive representation of high-dimensional MTS. Such visualizations in 2-D for the two controls used for illustration of the technique can be found in the right-hand side plot of Fig. 6. They show that the CSP is neatly represented by this model using separate states. This is a clean-cut indication that the change-points defining the onset and offset of the CSP are unambiguously detected and modelled by VB-GTM-TT.

A full report of the mean CSP durations of each subject obtained by both methods is provided in Table 2. It reveals that both methods estimate very similar durations of the CSP for all subjects but one, namely S14. This is an interesting result for the following reasons: First, it overall corroborates our initial hypothesis: that for data likely not to be contaminated by measurement noise, such as the controls under study, there is not much differential advantage in using the VB-GTM-TT-based *wpIV*. In other words, these cases are simple enough for the CSP duration to be easily estimated by any reliable method. In any case, the similarity of the estimations indicate that the manifold learning method is yielding accurate estimations. Second, and taking our attention back to control S14, the data corresponding to this subject (see them represented in Fig. 7), include many trials where the information about muscle contraction after the CSP was not properly acquired. As a result, the VB-GTM-TT-based method does not establish an offset estimation for the CSP, while DM detects an inexistent one.

Table 2
Table containing the mean of the estimated duration of the CSP for each control subject, using DM (central column) and VB-GTM-TT-based *wpIV* (right hand-side column).

Subject	DM (ms)	*wpIV* (ms)
S01	191	187
S02	283	284
S03	180	171
S04	259	263
S05	283	293
S06	260	261
S07	236	235
S08	236	239
S09	199	184
S10	288	277
S11	189	200
S12	258	245
S13	166	165
S14	157	203

4.3.4. Experiments with stroke patients

The final stage of our experiments concerns the analysis of data corresponding to pathological patients. These patients often have many difficulties to maintain a stable contraction of the muscle on the affected hand, and EMG spindles are registered during the CSP because of slow disruptions of inhibition processes. Also, the time necessary for the montage of the TMS and for data acquisition protocol is relatively high, causing discomfort and tiredness in the patients, making the task difficult. Given the circumstances, it seems probable that raw data will be contaminated by different types of artifacts, making the estimation of the CSP duration far more difficult than for control subjects.

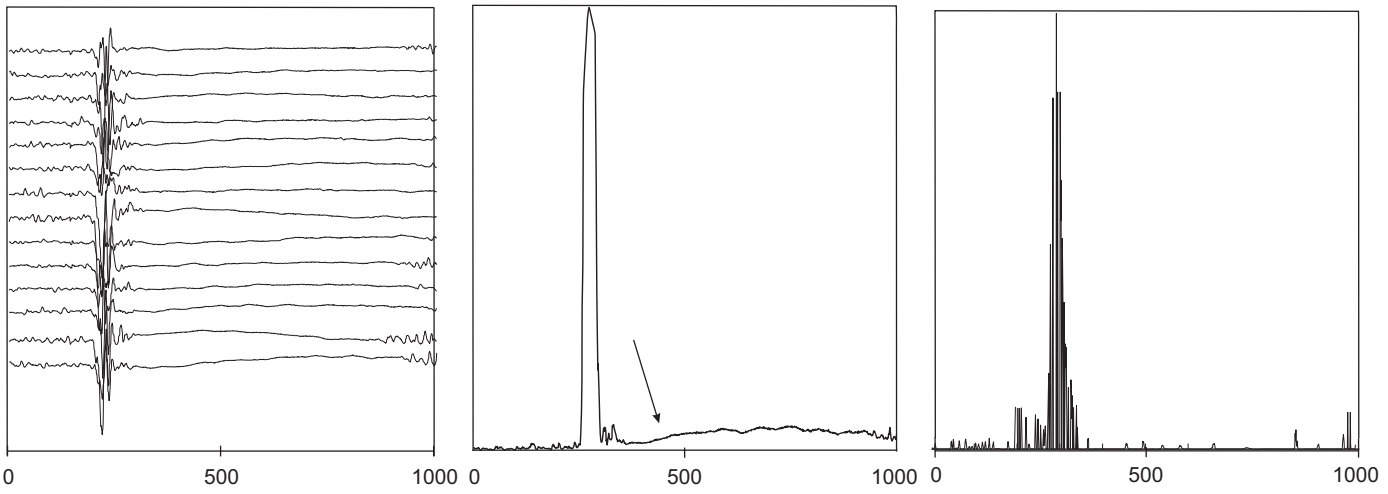

Fig. 7. (Left) The EMG time series for control subject S14. As can be observed, the return of voluntary contraction of the muscle was not acquired. (Center) Output of signal squaring by DM. The arrow marks the wrong offset of CSP estimated by DM. (Right) *wpIV* of the data; the method cannot find any offset of the CSP.

Our hypothesis now (once both DM and VB-GTM-TT-based *wpIV* have been evaluated with artificial data and real EMG from control subjects) is that the VB-GTM-TT-based *wpIV* method will have a differential advantage in the measurement of the CSP for these data, because of their noisy nature.

The mean CSP durations for each subject, obtained both by DM and the VB-GTM-TT-based *wpIV* are listed in full in Table 3. In contrast to the results obtained with control subjects, the results obtained by both methods with stroke rehabilitation patients are very different, as expected. In this case, Cornbach's alpha test produced a value of similarity of 0.53. Significant values for the *t*-test were found ($t(13) = -2.42$, $p < 0.03$), indicating significant differences between the estimations obtained by both methods. It must be noted, though, that in two cases, the VB-GTM-TT-based *wpIV* was not able to establish an offset time for the CSP (Fig. 8).

Table 3
Table containing the mean of the CSP of each participant using DM (central column) and the VB-GTM-TT-based *wpIV* (right hand-side column).

Subject	DM (ms)	*wpIV* (ms)
P01	126	206
P02	263	292
P04	144	160
P05	291	259
P07	–	–
P09	286	315
P10	246	341
P11	–	–

As for control subjects, illustrative results are presented in Fig. 9 for one stroke patient. All data trials and the estimation of the CSP duration are shown on the left-hand side; the calculated *wpIV* over time is shown on the center; while the low-dimensional VB-GTM-TT representation of the data is shown on the right-hand side.

The *wpIV* provides a clean-cut delimitation of the CSP that allows the unambiguous estimation of its duration. The 2-D visualization shows that the CSP is accordingly described almost in full by separate model states.

Let us also illustrate the difference of applying either the proposed VB-GTM-TT-based method, or DM to two stroke patients. Results are shown in Fig. 10: raw data for all trials (left); results of the application of DM (center) and of VB-GTM-TT (right). In both cases, the DM estimation of the duration of the CSP places the offset time of the silent period in a noise-affected location of the refractory period. Also in both cases, our proposed method instead marks the end of the silent period in a correct way, which is coherent with the visual output of the method.

These results confirm that DM does not seem to be a reliable tool to measure the CSP in EMG acquisition from stroke patients, possibly because of the large amount of noise present in the data. They also suggest that the VB-GTM-TT-based *wpIV* is a robust method for CSP analysis in noise-contaminated EMG.

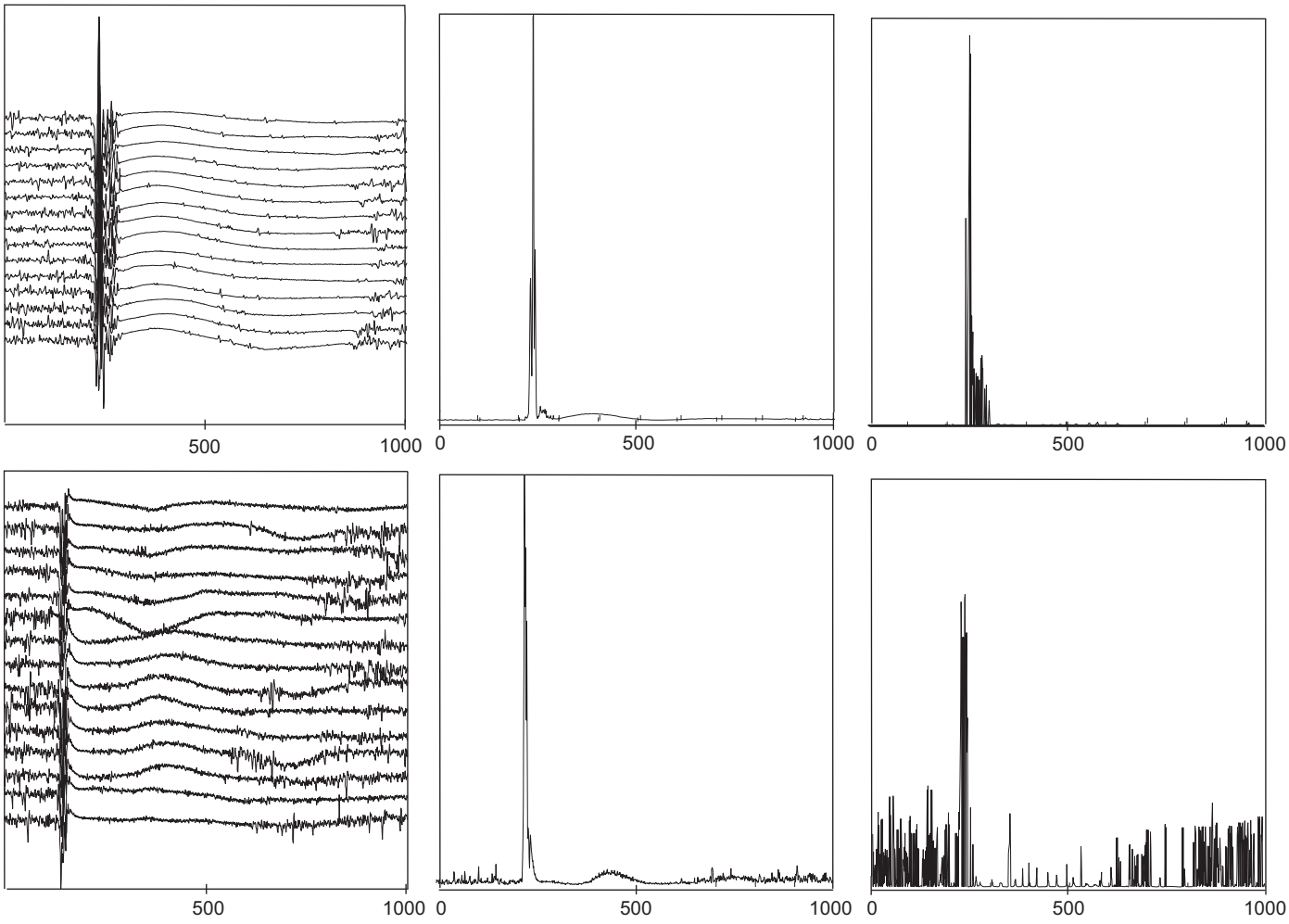

Fig. 8. (Left) The EMG (15 trials) for subjects P11 and P07. Representation as in the previous figure. It is clear that for the P07 patient (top), the return of voluntary contraction of the muscle was not properly acquired in several trials. As a result, the VB-GTM-TT-based method was not able to estimate an offset time for the CSP.

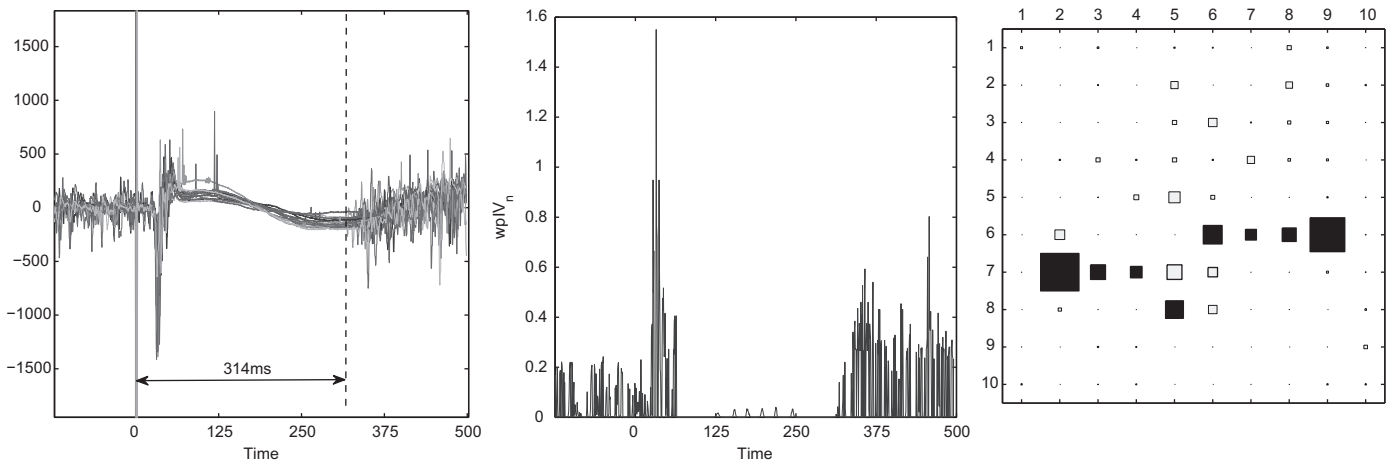

Fig. 9. Example of stroke patient. Representation as in Fig. 6.

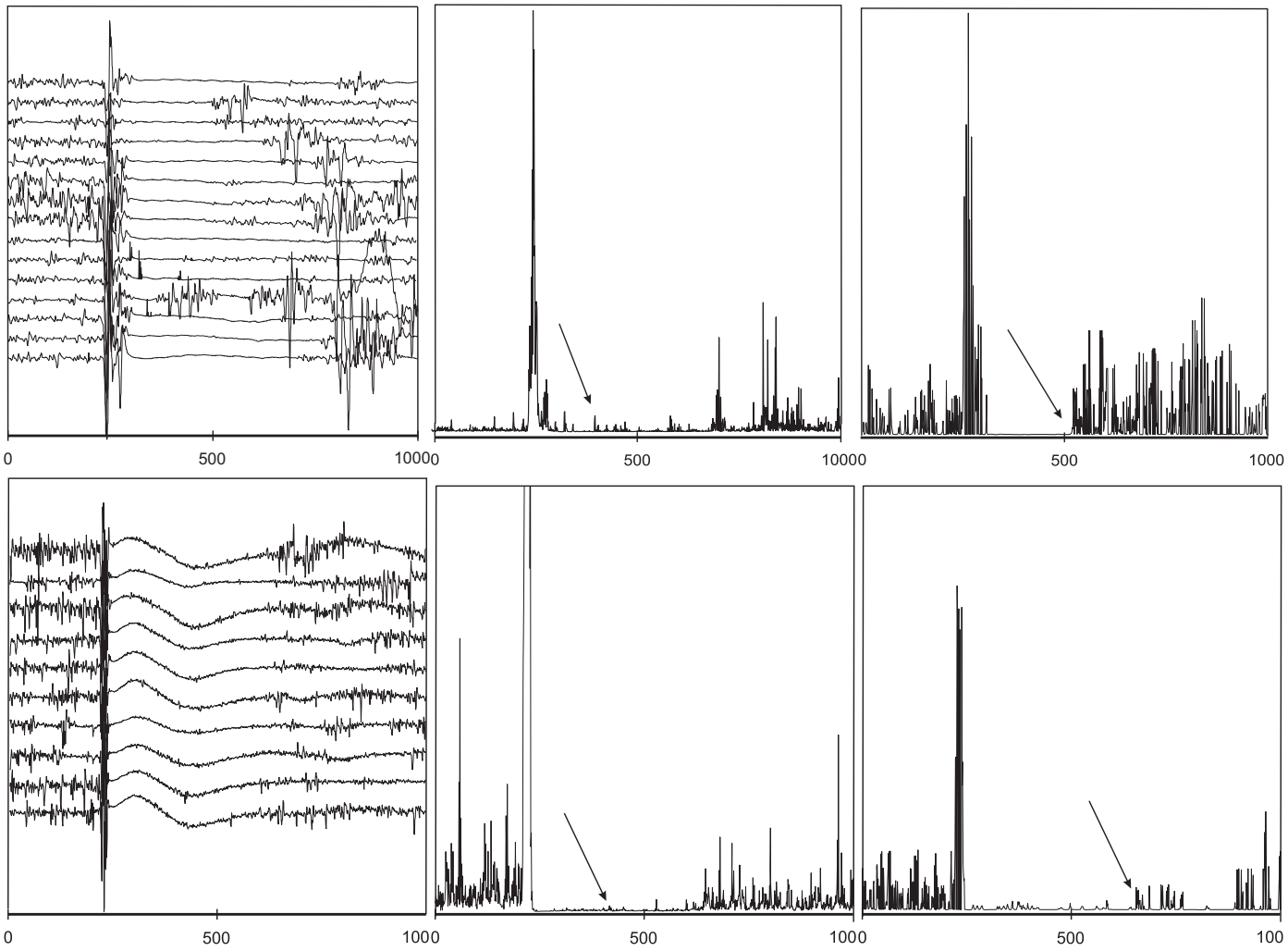

Fig. 10. Comparison between DM and *wpIV* in two stroke patients. (Left) 15 EMG trials acquired maintaining voluntary contraction of the muscle. (Center) Signal after application of DM. (Right) *wpIV* results. The arrow marks the estimation of the CSP offset in each method.

5. Conclusions

The CSP is known to be a key feature of EMG recordings from subjects affected by many neurological and psychiatric disorders. The CSP in such patients is often abnormal, reflecting altered cortical inhibition. For this reason, the accurate determination of the duration of the CSP is an important research target from a clinical viewpoint.

Traditionally, the CSP has been calculated using ad hoc techniques prone to subjective variability. Only recently, computer-based automated procedures for the estimation of its duration have become mainstream. The current standard procedures in

clinical practice, though, are limited mainly for their lack of robustness in the presence of noise. In this paper, we have put forward a novel method for the analysis of the CSP in EMG MTS. It is based on the robust detection of change points in the EMG signal using a statistical machine learning method of the manifold learning family.

The proposed index of variability based on the VB-GTM-TT manifold learning model has shown its ability to adequately detect change-points in the EMG signal through a battery of experiments. These experiments have been carried out both in artificially generated MTS and in real EMG signal.

The performances of the VB-GTM-TT-based method and DM, which is the current standard in the field, were compared. The results for VB-GTM-TT were consistently more accurate than those of DM in the estimation of the CSP in data contaminated by noise.

Real EMG data of control healthy subjects were subsequently used to test the new proposed method. This data is supposed to be almost noise – and acquisition artifacts – free. For this reason, we hypothesized that both compared methods should perform similarly. The results corroborated such hypothesis.

Finally, real EMG data acquired from stroke patients were analyzed. Both methods were applied to measure CSP duration on pathological data. Results provided some important evidence: As expected, the estimations of both methods differed substantially. Since the results obtained by DM are not coherent with what the data suggest through direct visualization, these experiments support the previous evidence that the *wpIV* measure behaves robustly in the presence of noise, while DM fails to provide an appropriate estimation.

In this study, the proposed method has been applied to data acquired from stroke patients, but many other clinical fields are currently interested in the study of inhibition phenomena as measured through EMG. Future research using this method could target, for instance, the problem of focal dystonia, a neurological condition affecting a muscle or group of muscles in a part of the body causing an undesirable muscular contraction or twisting. Inhibition is also a parameter related to the diagnosis and prognosis of Parkinson and Huntington diseases [49], which are the cause of tremoring and loss of muscle control that make the CSP measurement difficult.

Acknowledgment

This research was partially funded by Spanish MICINN R+D Plan TIN2009-13895-C02-01 project.

References

[1] Y. Terao, Y. Ugawa, Basic mechanisms of TMS, J. Clin. Neurophysiol. 19 (4) (2002) 322–343.
[2] J. Liepert, K. Haevernick, C. Weiller, A. Barzel, The surround inhibition determines therapy-induced cortical reorganization, Neuroimage 32 (3) (2006) 1216–1220.
[3] J. Liepert, Motor cortex excitability in stroke before and after constraint-induced movement therapy, Cogn. Behav. Neurol. 19 (1) (2006) 41–47.
[4] Z. Daskalakis, G. Molnar, B. Christensen, A. Sailer, T. Fitzgerald, R. Chen, An automated method to determine the transcranial magnetic stimulation-induced contralateral silent period, Clin. Neurophysiol. 114 (2003) 938–944.
[5] N.K.K. King, A. Kuppuswamy, P.H. Strutton, N.J. Daver, Estimation of cortical silent period following transcranial magnetic stimulation using a computerised cumulative sum method, J. Neurosci. Meth. 150 (1) (2006) 96–114.
[6] C.A. Rábago, J.L. Lancaster, S. Narayana, W. Zhang, P.T. Fox, Automated-parameterization of the motor evoked potential and cortical silent period induced by transcranial magnetic stimulation, Clin. Neurophysiol. 120 (8) (2009) 1577–1587.
[7] B. Dobkin, Rehabilitation after stroke, New Engl. J. Med. 352 (2005) 1677–1684.
[8] G. Kwakkel, Effects of augmented exercise therapy time after stroke: a meta-analysis, Stroke 35 (2004) 2529–2539.
[9] S. Schneider, P. Schoenle, E. Altenmueller, T. Muente, Using musical instruments to improve motor skill recovery following a stroke, J. Neurol. 10 (2007) 1339–1346.
[10] M. Hallet, Transcranial magnetic stimulation: a primer, Neuron 55 (1) (2007) 187–199.
[11] M. Kobayashi, A. Pascual-Leone, Transcranial magnetic stimulation in neurology, Lancet Neurol. 2 (2003) 145–156.
[12] W. Triggs, K. Rosler, A. Truffert, J. Mayers, Motor inhibition and excitation are independent effects of magnetic cortical stimulation, Ann. Neurol. 32 (1992) 345–351.
[13] A. Berardelli, Transcranial magnetic stimulation in movement disorders, Clin. Neurophysiol. 51 (1999) 276–280.
[14] J. Classen, A. Schnitzler, F. Bonjofski, The motor syndrome associated with exaggerated inhibition within the primary motor cortex of patients with hemiparetic, Brain 120 (1997) 605–619.
[15] R. Traversa, P. Cicinelli, M. Olivery, M. Filippi, P. Rossini, Neurophysiological follow-up of motor cortical output in stroke patients, Clin. Neurophysiol. 111 (2000) 1695–1703.
[16] P. Cicinelli, R. Traversa, P. Rossini, Post-stroke reorganization of brain motor output to the hand: a 2–4 month follow-up with focal magnetic transcranial magnetic stimulation, Electroencephalogr. Clin. Neurophysiol. 105 (1997) 438–450.
[17] H. Foltys, T. Krings, I. Meister, R. Sparing, R. Topper, Motor representation in patients rapidly recovering after stroke: a functional magnetic resonance imaging and transcranial magnetic stimulation study, Clin. Neurophysiol. 114 (2003) 2404–2415.
[18] F. Fregni, P. Boggio, C. Mansur, A.P. Leone, Transcranial direct current stimulation of the unaffected hemisphere in stroke patients, Neuroreport 16 (2005) 1551–1555.
[19] C.M. Bishop, Latent Variable Models, MIT Press, 1999.
[20] M. Svensén, GTM: the generative topographic mapping, Ph.D. Thesis, Aston University, UK, 1998.
[21] I.T. Jolliffe, Principal Component Analysis, Springer-Verlag, New York, 1986.
[22] T. Hastie, Principal curves and surfaces, Technical Report, Department of Statistics, Stanford University, 1984.
[23] M.A. Kramer, Nonlinear principal components analysis using autoassociative neural networks, AIChe J. 37 (2) (1991) 233–243.
[24] C. Cortes, V. Vapnik, Support-vector networks, Mach. Learn. 20 (1995) 273–297.
[25] D.J. Bartholomew, Latent Variable Models and Factor Analysis, Charles Griffin and Co. Ltd, London, 1987.
[26] D.N. Lawley, A.E. Maxwell, Factor Analysis as a Statistical Method, second ed., Butterworth & Co., London, 1971.
[27] C.M. Bishop, M. Svensén, C.K.I. Williams, GTM: the generative topographic mapping, Neural Comput. 10 (1) (1998) 215–234.
[28] T. Kohonen, Self-organizing Maps, third ed., Springer-Verlag, Berlin, 2001.
[29] P. Tino, I. Nabney, Hierarchical GTM: constructing localized nonlinear projection manifolds in a principled way, IEEE Trans. Pattern Anal. Mach. Intell. 24 (5) (2002) 639–656.
[30] I. Olier, A. Vellido, Comparative assessment of the robustness of missing data imputation through generative topographic mapping, Lecture Notes in Computer Science, vol. 3512, 2005, pp. 787–794.
[31] C.M. Bishop, M. Svensén, C.K.I. Williams, Developments of the generative topographic mapping, Neurocomputing 21 (1–3) (1998) 203–224.
[32] A. Vellido, W. El-Deredy, P.J.G. Lisboa, Selective smoothing of the generative topographic mapping, IEEE Trans. Neural Network 14 (4) (2003) 847–852.
[33] C.M. Bishop, M.E. Tipping, A hierarchical latent variable model for data visualization, IEEE Trans. Pattern Anal. Mach. Intell. 20 (3) (1998) 281–293.
[34] M. Girolami, Latent variable models for the topographic organisation of discrete and strictly positive data, Neurocomputing 48 (2002) 185–198.
[35] A. Vellido, P.J.G. Lisboa, D. Vicente, Robust analysis of MRS brain tumour data using t-GTM, Neurocomputing 69 (7–9) (2006) 754–768.
[36] R. Cruz, A. Vellido, Semi-supervised geodesic generative topographic mapping, Pattern Recognition Lett. 31 (2010) 202–209.
[37] C.M. Bishop, G. Hinton, I. Strachan, GTM through time, in: IEE Fifth International Conference on Artificial Neural Networks, Cambridge, UK, 1997, pp. 111–116.
[38] L. Rabiner, A tutorial on hidden Markov models and selected applications in speech recognition, Proceedings of the IEEE 77 (2) (1989) 257–285.
[39] I. Olier, A. Vellido, On the benefits for model regularization of a variational formulation of GTM, in: Proceedings of the IEEE International Joint Conference on Neural Networks (IJCNN 2008), Hong Kong, 2008, pp. 1568–1575.
[40] I. Olier, A. Vellido, A variational formulation for GTM through time, in: Proceedings of the IEEE International Joint Conference on Neural Networks (IJCNN 2008), Hong Kong, 2008, pp. 516–521.
[41] L. Baum, J. Egon, An inequality with applications to statistical estimation for probabilistic functions for a Markov process and to a model for ecology, Brit. Am. Meteorol. Soc. 73 (1967) 360–363.
[42] C. Chatfield, Time Series Forecasting, Chapman & Hall/CRC Press, 2000.
[43] G. Zhang, B. Patuwo, M. Hu, Forecasting with artificial neural networks: the state of the art, Int. J. Forecasting 14 (1) (1998) 35–62.
[44] A. Kabán, M. Girolami, A dynamic probabilistic model to visualise topic evolution in text streams, J. Intell. Inf. Syst. 18 (2–3) (2002) 107–125.
[45] I. Olier, Variational Bayesian algorithms for the generative topographic mapping and its extensions, Ph.D. Thesis, Universitat Politècnica de Catalunya, Spain, 2008.
[46] M. Beal, Variational algorithms for approximate Bayesian inference, Ph.D. Thesis, The Gatsby Computational Neuroscience Unit, University College London, 2003.

[47] I. Olier, A. Vellido, Advances in clustering and visualization of time series using GTm through time, Neural Networks 21 (7) (2008) 904–913.
[48] L. Cronbach, Coefficient alpha and the internal structure of test, Psychometrika 3 (16) (1951) 297–334.
[49] G. Koch, L. Brusa, P. Stanzione, Cerebellar magnetic stimulation decreases levodopa-induced dyskinesias in parkinson disease, Neurology 72 (2009) 113–119.

Iván Olier is currently a Marie Curie research fellow at the School of Psychological Sciences, The University of Manchester, UK. Previously, he was a postdoctoral fellow at the Institute of Neurosciences, *Universitat Autdnoma de Barcelona*, Spain, during the period 2009–2010. He received his Ph.D. in Computer Science from the *Universitat Politècnica de Catalunya*, Barcelona, Spain, in 2008. His research interests include Bayesian modeling of cognitive processes, statistical machine learning and biomedicine.

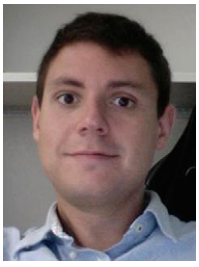

Julià Amengual received his degree in Mathematics from the Department of Mathematics and Computer Sciences of the University of Balearic Islands in 2007. He completed his M.Sc. in Artificial Intelligence at *Universitat Politècnica de Catalunya*, Barcelona, Spain, in 2010. He is currently a member of the Cognition and Brain Plasticity Unit located at Bellvitge Hospital (*Universitat de Barcelona*) as a Ph.D. student. Research interests include brain plasticity and neurorehabilitation in acute and chronic stroke patients; automated methods of calculation of EMG parameters, EEG time–frequency analysis and transcranial magnetic stimulation.

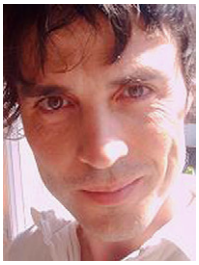

Alfredo Vellido received his degree in Physics from the Department of Electronics and Automatic Control of the University of the Basque Country (Spain) in 1996. He completed his Ph.D. at Liverpool John Moores University (UK) in 2000. After a few years of experience in the private sector, he briefly joined Liverpool John Moores University again as senior research officer. Following a *Ramón y Cajal* research fellowship, he is currently assistant professor at *Universitat Politècnica de Catalunya* in Barcelona, Spain. Research interests include, but are not limited to, pattern recognition, machine learning and data mining, as well as their application in medicine, market analysis, ecology, and e-learning, on which subjects he has published widely.